

# $\Lambda\Lambda$ INTERFEROMETRY IN $(K^-, K^+)$ AND $AA$ REACTIONS

Akira Ohnishi<sup>a</sup>, Yuichi Hirata<sup>a</sup>, Yasushi Nara<sup>b</sup>, Shoji Shinmura<sup>c</sup> and Yoshinori Akaishi<sup>d</sup>

*a Division of Physics, Graduate School of Science, Hokkaido University,  
Sapporo 060-0810, Japan*

*b Advanced Science Research Center, Japan Atomic Energy Research Institute,  
Tokai, Ibaraki 319-11, Japan*

*c Faculty of Engineering, Gifu University, Yanagido 1-1, Gifu 501-11, Japan*

*d Institute of Particle and Nuclear Study, KEK (Tanashi Branch),  
Midorimachi 3-2-1, Tanashi 188, Japan*

We analyze the invariant mass spectrum of  $\Lambda\Lambda$  in  $^{12}\text{C}(K^-, K^+\Lambda\Lambda)$  reaction at  $P(K^-) = 1.65$  GeV/ $c$  by using a combined framework of IntraNuclear Cascade (INC) model and the correlation function technique. The observed enhancement at low-invariant masses can be well reproduced with attractive  $\Lambda\Lambda$  interactions with the scattering length either in the range  $a = -6 \sim -4$  fm (no bound state) or  $a = 7 \sim 12$  fm (with bound state) within the present theoretical treatment. We also discuss  $\Lambda\Lambda$  correlation functions in central relativistic heavy-ion collisions as a possible way to eliminate this discrete ambiguity.

## 1 Introduction

Extracting hyperon-hyperon ( $YY$ ) interactions is one of the most challenging current problems in nuclear physics. It provides us of an opportunity to verify various ideas on baryon-baryon interactions such as the flavor  $\text{SU}(3)$  symmetry.  $YY$  interactions may also modify the properties of neutron stars, in which abundant hyperons are expected to exist. However, it is very difficult to determine them experimentally. For example,  $YY$  scattering experiments, which can directly access  $YY$  interactions, require a collider machine with a very compact geometry because of their short lifetimes. On the other hand, only three double  $\Lambda$  nuclei, from which informations of the low-energy  $^1\text{S}_0$   $\Lambda\Lambda$  interaction are available, are found in these 35 years.<sup>1,2,3</sup> Therefore, other ways to extract  $YY$  interactions with various combination of hyperons at various energies have been desired so far.

One of these ways is opened up by a recent measurement of the invariant mass spectrum of  $\Lambda\Lambda$  pair in  $^{12}\text{C}(K^-, K^+\Lambda\Lambda)$  reaction by Ahn et al.(KEK-E224 collaboration).<sup>4</sup> The measured invariant mass spectrum shows a clear enhancement at around the threshold of  $\Lambda\Lambda$  compared to those calculated with the IntraNuclear Cascade (INC) model<sup>5</sup> and to those estimated from the three-body phase volume of  $^{11}\text{B}_{g.s.}\Lambda\Lambda$  with the aid of experimentally measured  $K^+$  spectrum.

The invariant mass spectra, or two-particle momentum correlations, have been widely used to evaluate the source size when the final state interactions are negligible or well-known.<sup>6,7,8,9,10,11,12</sup> For (practically) non-interacting bosons such as  $\gamma\gamma$ , the correlation function tends towards two at small relative momentum, and the enhanced range in the momentum is inversely related to the source size. This enhancement purely comes from the spatially symmetric relative wave function of two bosons. For fermions, the enhancement at low relative momentum goes to one half, if we ignore final state interactions and assume a statistical spin distribution

(singlet:triplet = 1:3). Without the final state interaction, the enhancement cannot exceed two, even if we assume that the spin singlet identical fermion pairs are dominant. Therefore, the measured enhancement in the invariant mass spectrum, which seems to be much larger than two, strongly suggests the necessity of the *attractive* final state interaction of  $\Lambda\Lambda$ .

The two particle momentum correlation between baryons are significantly affected by final state interactions and reaction mechanisms. For example, the proton-proton correlation data shows a depression at small momenta (Coulomb pocket) and an enhancement at around the  ${}^2\text{He}$  resonance. In addition, the initial state correlation of spin is known to be important in light-ion induced reactions.<sup>13</sup> Since two-particle momentum correlations are evaluated from the source function and the relative wave function, it is necessary to invoke a well established strong interaction and a dynamical model for the understanding of baryon-baryon correlation. In other words, if we have a *reliable* dynamical model, it would be possible to extract the information on the interaction between the measured particle pair. Actually, precise few-body calculations made it possible to extract neutron-neutron effective range from the particle momentum correlation data.<sup>14</sup>

In this work, first we apply the correlation function technique to the  $\Lambda\Lambda$  invariant mass spectrum data, and try to determine  $\Lambda\Lambda$  interaction at low energies, by using a source function generated by the IntraNuclear Cascade (INC) model,<sup>5</sup> which well reproduce inclusive ( $K^-$ ,  $K^+$ ) spectra. In  ${}^{12}\text{C}(K^-, K^+\Lambda\Lambda)$  reactions, the leading particle creates two  $\Lambda$  at a small distance. This small source size emphasizes the effects of final state interactions at low energies, and a large enhancement is realized. However, we find that the invariant mass spectrum in this reaction is not sensitive to the long range behavior in the continuum wave function, such as the orthogonality to a bound state wave function. Hence the observed enhancement at low energies can be well reproduced with attractive  $\Lambda\Lambda$  interactions having the scattering length either in the range  $a = -6 \sim -4$  fm (no bound state) or  $a = 7 \sim 12$  fm (with bound state).

In order to distinguish whether two lambdas bound or not, it is helpful to utilize reactions with large source size. We then show the calculated results of  $\Lambda\Lambda$  correlation functions in relativistic heavy-ion collisions at BNL-AGS, CERN-SPS, and BNL-RHIC energies. The results show that the correlation functions in heavy-ion collisions are sensitive to the existence of bound state in the relative momentum range  $q < 40$  MeV/ $c$ .

## 2 Invariant Mass Spectrum in ${}^{12}\text{C}(K^-, K^+)$ Reaction

The inclusive spectra of ( $K^-, K^+$ ) reaction on various targets<sup>15</sup> can be explained well by the INC model,<sup>5</sup> as a sum of following contributions; (a) quasi-free  $\Xi^{(*)}$  production, (b) heavy-meson ( $\phi/a_0/f_0$ ) production followed by its decay,<sup>17</sup> and (c) various two-step processes.<sup>16</sup> The predicted reaction mechanism in this model was experimentally verified recently.<sup>16</sup> In this work, we use this INC model to generate a hyperon source function. As for the baryon momentum spectra, however, mean field effects are also important. Thus we include them as external potentials with the depths of  $-40$ ,  $-30$ ,  $-10$ , and  $-16$  MeV for  $N$ ,  $\Lambda$ ,  $\Sigma$ , and  $\Xi$ <sup>18</sup> baryons, respectively.

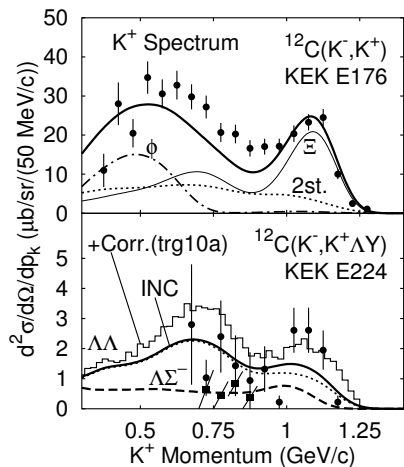


Figure 1: Calculated momentum spectra of  $K^+$  particle in  $^{12}\text{C}(K^-, K^+)$  (upper panel) and  $^{12}\text{C}(K^-, K^+\Lambda Y)$  (lower panel) reactions are compared with experimental data.<sup>4,15,16</sup>

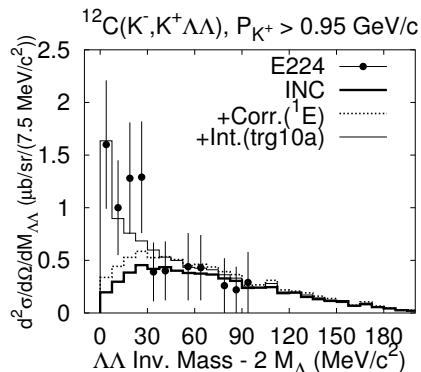


Figure 2: Calculated  $\Lambda\text{-}\Lambda$  invariant mass spectrum by using INC model without (thick) and with (thin) correlation effects are compared with data (solid circles).<sup>4</sup>

In addition, we have adopted the hyperon-nucleon scattering and conversion cross sections calculated with the Nijmegen model D potential.<sup>19</sup> For  $S = -2$  collisions, we fixed the hardcore radius to be  $r_c = 0.5$  fm.

In Fig. 1, we compare the calculated  $K^+$  momentum spectra in inclusive ( $K^-, K^+$ ) and coincidence ( $K^-, K^+\Lambda Y$ ) reactions with experimental data.<sup>4,15,16</sup> The calculated results (thick solid curve) well explains the data except for the underestimate of two lambda production at around  $P_{K^+} \simeq 1.1$  GeV/c, and the underestimate of inclusive  $K^+$  spectrum at intermediate momenta,  $0.5 \leq P(K^+) \leq 0.9$  GeV/c. Since the  $\Lambda\Lambda$  invariant mass spectrum is measured in the high momentum range of  $K^+$ ,  $P(K^+) \geq 0.95$  GeV/c, we do not care the latter underestimate in the following discussion of this paper.

The underestimate of coincidence cross section ( $K^-, K^+\Lambda\Lambda$ ) is concentrated in the low invariant mass region of  $\Lambda\Lambda$ , as shown in Fig. 2. This is as expected, since the correlation caused by the final state interaction modify the invariant mass spectrum at low mass region most effectively.

The enhancement of the two-particle momentum spectrum has been extensively studied in the context of correlation function. For example, in the correlation function formula,<sup>12</sup> the probability to find particle pair at momenta  $\vec{p}_1$  and  $\vec{p}_2$  reads,

$$P(\vec{p}_1, \vec{p}_2) = \int d^4x_1 d^4x_2 S_{12}(\vec{p}_1, x_1, \vec{p}_2, x_2) \left| \psi^{(-)}(\vec{r}_{12}; \vec{k}) \right|^2, \quad (1)$$

$$\vec{r}_{12} = \vec{r}_1 - \vec{r}_2 + \vec{P}(t_2 - t_1)/2m, \quad (2)$$

$$\vec{P} = \vec{p}_1 + \vec{p}_2, \vec{k} = \frac{1}{2\hbar}(\vec{p}_1 - \vec{p}_2), \quad (3)$$

where  $\vec{r}_{12}$  is the relative distance of two particles at particle creation,  $S_{12}$  denotes

Table 1: Two-range Gaussian (trg)  $\Lambda\Lambda$  potential parameters which give a local  $\chi^2$  minimum for a given range parameter  $\mu_l$ . The shorter range  $\mu_s = 0.45$  fm is fixed for simplicity. For each parameter set, the scattering length  $a$ , the effective range  $r_{\text{eff}}$ , the reduced residual error  $\tilde{\chi}^2 \equiv \chi^2/\text{DOF}$ , and the binding energy are also shown.

	$\mu_l$ (fm)	$\mu_s$ (fm)	$v_l$ (MeV)	$v_s$ (MeV)	$a$ (fm)	$r_{\text{eff}}$ (fm)	$\tilde{\chi}^2$	B.E. (MeV)
trg06a	0.60	0.45	-900.0	1440.0	-4.4	1.6	0.34	U.B.
trg08a	0.80	0.45	-230.0	470.0	-5.0	1.8	0.36	U.B.
trg10a	1.00	0.45	-105.0	200.0	-6.2	2.0	0.39	U.B.
trg06b	0.60	0.45	-950.0	1310.0	7.5	1.2	0.38	0.72
trg08b	0.80	0.45	-270.0	410.0	8.5	1.3	0.40	0.56
trg10b	1.00	0.45	-135.0	210.0	11.5	1.6	0.43	0.29

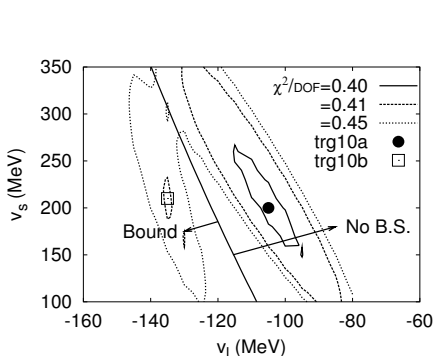


Figure 3:  $\chi^2$  surface in the potential strength plane,  $(v_l, v_s)$ , for  $\mu_l = 1.0$  fm. There are two local minima, trg10a and trg10b, shown in a solid point and a open square, respectively.

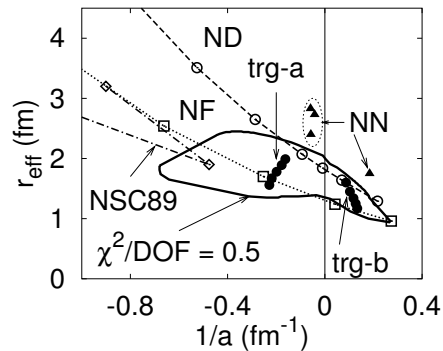


Figure 4: Extracted  $\Lambda\Lambda$  scattering parameters. Fitted two-range gaussian potentials (solid circles) are compared with Nijmegen models (open marks). Inside the thick solid line, potential with  $\tilde{\chi}^2 \leq 0.5$  exists in the range  $0.6 \leq \mu_l \leq 1.0$  fm.

the source function, and the wave function  $\psi^{(-)}$  is chosen to have the outgoing relative momentum. In this work, we limit ourselves to working in a single channel description of  $\Lambda\Lambda$ , and assume that two  $\Lambda$  particles are in their spin singlet state. Then, the relative wave function of  $\Lambda\Lambda$  at small relative momentum is simplified as follows.

$$\psi^{(-)}(\vec{r}; \vec{k}) \simeq \sqrt{2} \left[ \cos(\vec{k} \cdot \vec{r}) - j_0(kr) + e^{-i\delta_0} u_0(r; k) \right]. \quad (4)$$

Based on these formula, we have calculated the  $\Lambda\Lambda$  invariant mass spectrum including the correlation effects. In INC, we have specified the particle "creation" point to be the last point where the  $\Lambda$  particle is created by the leading particle or it collides with other nucleons. Here we have used phenomenological  $\Lambda\Lambda$  potentials parametrized in a two-range Gaussian form,  $V_{\Lambda\Lambda}(r) = v_l \exp(-r^2/\mu_l^2) + v_s \exp(-r^2/\mu_s^2)$ . As shown by the thin histogram in Fig. 2, the enhancement at low invariant masses can be reproduced with an appropriate potential, although the second "peak" around 25 MeV is difficult to explain. At higher invariant masses the

correlation effects are washed out by the oscillation of  $|\psi|^2$  in the source spreading upto around  $r_{12} \simeq 5$  fm.

Some reader may doubt that the enhancement at low energies are too large to explain by the correlation, since the correlation functions (enhancements) are usually less than two, and  $pp$  correlations are almost zero at low momenta. However, it is the Coulomb interaction that suppresses  $pp$  correlation at low energies, and the measured  $nn$  correlation functions in heavy-ion collisions exhibit a strong maximum,  $C(q \rightarrow 0) > 5$ , at zero energies.<sup>20</sup>

We have searched for the  $\chi^2$  local minima in the  $(v_l, v_s)$  plane for a given longer range parameter,  $\mu_l = 0.6 \sim 1.0$  fm (Table 1). There are generally two  $\chi^2$  local minima as shown in Fig. 3. In Fig. 4, we compare the extracted  $\Lambda\Lambda$  potentials with the Nijmegen models.<sup>19,21,22</sup> From this comparison, model ND<sup>19</sup> (NF<sup>21</sup>) with the hardcore radius  $r_c \simeq 0.50(0.46)$  fm, and model NSC89<sup>22</sup> with the cutoff mass  $M_{cut} \simeq 920$  MeV are expected to give reasonable enhancement in the  $\Lambda\Lambda$  invariant mass spectrum.

### 3 Do Two Lambdas Bound ?

As shown in Table 1, all the best fit parameters (trg-a) give negative scattering length ( $\delta_0 \sim -ak$ ), implying that there is no bound state. However, there is another local minimum (trg-b) in the region where there is a bound state,  $a > 0$ . This double-well structure appears because the enhancement is described by the wave function squared. With the long wave approximation, the wave function becomes essentially a constant, then the correlation effect can be factorized as follows,<sup>14</sup>

$$P(\vec{p}_1, \vec{p}_2) \simeq 2F(k) P_c(\vec{p}_1, \vec{p}_2), \quad P_c = \int d^4x_1 d^4x_2 S_{12}, \quad F(k) = (1 - a/b)^2 - ck^2, \quad (5)$$

where  $b$  denotes the intrinsic range. There are two solutions of  $a$  giving the same enhancement at low energies,  $a \sim b \left(1 \pm \sqrt{F(0)}\right)$ . When the spectrum is enhanced at low energies,  $F(0) > 1$ , one of them is negative (no bound state) and the other becomes positive (with bound state).

This situation is shown in the upper panel of Fig. 5, where we show the (momentum integrated) source distribution, and the wave function in the  $^1S_0$  channel calculated with the potential parameters of trg10a and trg10b at asymptotic relative momenta of  $k = 0.4, 0.2, 0.1$  and  $0.01$  fm<sup>-1</sup>. All these momenta are in the range of the lowest energy bin of experimental data. Although there are some differences in the wave functions at extremely small momenta, we cannot distinguish them when integrated out over the momenta in the above range.

In order to overcome this problem and to distinguish these two kind of solutions, it may be helpful to use relativistic heavy-ion collisions, where the source size is much larger than that in  $(K^-, K^+)$  reaction and the long wave approximation would not work. For example, the scattering wave function have at least one node in the range  $r \leq a$  when a bound state exists, which suppresses the contribution at around  $r \sim a$  in two-particle correlations. Since this behavior of wave functions is robust and remains true at low momenta, we expect significant sensitivity to the existence of

$\Lambda\Lambda$  bound state if the source covers the range,  $3 \leq r_{12} \leq 15$  fm.

In order to generate relativistic heavy-ion collision events, we have applied a recently developed hadron-string cascade model named JAM<sup>23</sup> to reactions at AGS, SPS and RHIC energies. One of the good features of JAM is its wide energy range of applicability. For example, particle productions are modeled by the resonance production at low energies ( $\sqrt{s_{NN}} < 3.5$  GeV), soft string excitation upto around SPS energies, and multiple minijet production at higher energies. At AGS and SPS energies, this model has been shown to work well in describing  $m_T$  and rapidity distribution of  $p, \pi$  and  $K$  for various combination of projectile and targets.<sup>23</sup>

We have generated central collision events of Au+Au collisions at AGS and RHIC energies and S+S collisions at SPS energy. Generated source distributions at several relative momenta are shown in the lower panel of Fig. 5. These distributions cover the range where the difference of the wave function is clear.

In Fig. 6, we show the calculated  $\Lambda\Lambda$  correlation function,  $C(q)$ , in relativistic heavy-ion collisions with the above source function generated by using JAM. Here statistical spin distribution is assumed. As expected in the above discussion, two-particle correlations are suppressed at small momenta with trg10b and trg06b (with bound state) compared with trg10a (no bound state). When the source size is large enough (Au+Au collisions), the difference becomes larger. Especially, there is a qualitative difference in Au+Au collisions that the correlation function becomes smaller than unity when there is a bound state, while it has a maximum at zero relative momentum for interactions without bound state.

#### 4 Summary

In this paper, first we have analyzed the  $\Lambda\Lambda$  invariant mass spectrum in  $^{12}\text{C}(K^-, K^+ \Lambda\Lambda)$  reaction by using the classical source function generated by using the IntraNuclear Cascade (INC) model combined with the correlation function formula, which takes account of  $\Lambda\Lambda$  interaction. Within a single channel description of  $\Lambda\Lambda$ , and under the assumption that two lambdas are in their spin-singlet state, we limit the allowed range of  $\Lambda\Lambda$  scattering parameters. The observed enhancement at low-invariant masses can be well reproduced with attractive  $\Lambda\Lambda$  interactions with the scattering length either in the range  $a = -6 \sim -4$  fm (no bound state) or  $a = 7 \sim 12$  fm (with bound state) within the present theoretical treatment. The origin of this discrete ambiguity is discussed in the context of a long wave approximation.

Next we have discussed a possibility to use relativistic heavy-ion collisions as one of the ways to distinguish the  $\Lambda\Lambda$  potentials, which reproduce the invariant mass spectrum of  $\Lambda\Lambda$  equally well in  $(K^-, K^+)$  but have different sign of the scattering length. The key point is that the continuum wave function has to have at least one node in the range  $r \leq a$  if there is a bound state. We find that there appears a qualitative difference in the correlation function  $C(q)$ , for (really-)heavy-ion collisions, such as Au+Au, which have a large source size.

Although we can also see a similar difference in the correlation function in  $^{12}\text{C}(K^-, K^+)$  reaction, we cannot estimate the "uncorrelated" probability in this reaction. Two  $\Lambda$  particles are created by the same leading particle and dynamically correlated in  $(K^-, K^+)$  reactions. Therefore, we cannot define the correlation

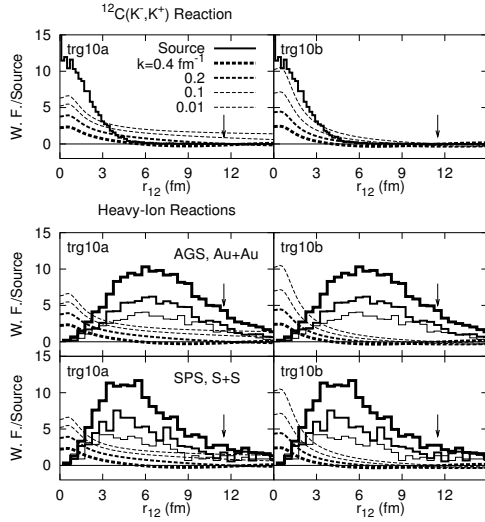


Figure 5:  $\Lambda\Lambda$  relative distance distribution in  $(K^-, K^+)$  reaction and central relativistic heavy-ion collisions at AGS, SPS, and RHIC energies. The wave functions in  $^1S_0$  channel at several momenta are also shown for trg10a (left) and trg10b (right).

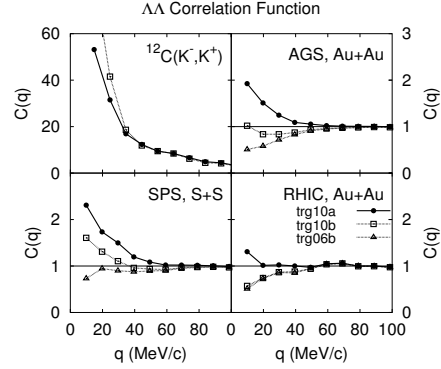


Figure 6:  $\Lambda\Lambda$  correlation function in  $(K^-, K^+)$  reaction and central relativistic heavy-ion collisions at AGS, SPS, and RHIC energies. The results with trg10a (solid circles) and trg10b (open squares) are compared.

coming from the  $\Lambda\Lambda$  interaction separately from this dynamical correlation.

As discussed at the meeting, there are still large ambiguities to be fixed in the theoretical models which generate source functions. For example, we have to estimate the cross sections of experimentally unknown processes, such as  $\eta N \rightarrow KY$ , which we estimated by applying the generalized Breit-Wigner formula at KEK energy,  $P(K^-) = 1.65 \text{ GeV}/c$ . At higher incident momentum such as in BNL-E906 experiment,<sup>24</sup> where the expected number of  $\Lambda\Lambda$  pairs exceeds the current data by around two order of magnitude, strings start to appear and it becomes more elaborate to estimate cross sections. However, we already have careful estimates of  $K^-N$  cross sections at this momentum for several channels.<sup>23</sup> In addition, we can in principle reduce the ambiguity by analyzing other cross sections such as  $(K^-, \pi)$  or  $(K^-, \Lambda)$ . Especially, it is necessary to analyze the inclusive  $\Lambda$  spectrum (Fig. 7) to verify various inputs of cascade models, before getting any decisive conclusions.

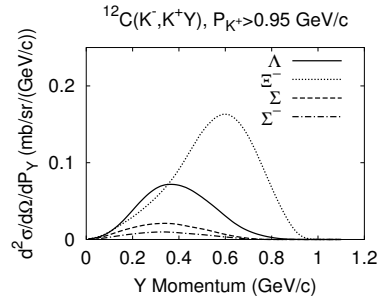


Figure 7: Hyperon momentum spectrum in  $^{12}\text{C}(K^-, K^+Y)$  reaction with the condition  $P(K^+) > 0.95 \text{ GeV}/c$ .

## Acknowledgments

The authors would like to thank Dr. J. K. Ahn and Prof. J. Randrup, and all the participants of this workshop for fruitful discussions. This work was supported in part by the Grant-in-Aid for Scientific Research (Nos. 07640365, 08239104 and 09640329) from the Ministry of Education, Science and Culture, Japan.

1. M. Danyz *et al.*, Nucl. Phys. **49** (1963), 121.
2. D. J. Prowse, Phys. Rev. Lett. **17** (1966), 782.
3. S. Aoki *et al.* (KEK-E176 collaboration), Prog. Theor. Phys. **85** (1991), 1287.
4. J.K. Ahn *et al.* (KEK-E224 collaboration), Phys. Lett. **B444** (1998), 267.
5. Y. Nara, A. Ohnishi, T. Harada, and A. Engel, Nucl. Phys. **A614** (1997), 433.
6. R. Hanbury Brown and R.Q. Twiss, Philos. Mag. **45** (1954), 663; Nature **177** (1956), 27; Nature **178** (1956), 1046.
7. G. Goldhaber *et al.*, Phys. Rev. Lett. **3** (1959), 181; Phys. Rev. **120** (1960), 300.
8. E. V. Shuryak, Phys. Lett. **B44** (1973), 387.
9. S. Pratt, Phys. Rev. Lett. **53** (1984), 1219.
10. S. E. Koonin, Phys. Lett. **B70** (1977), 43.
11. W. G. Gong *et al.*, Phys. Rev. C **43** (1991), 781.
12. W. Bauer, C.K. Gelbke, and S. Pratt, Annu. Rev. Nucl. Part. Sci. **42** (1992), 77.
13. F. Zhu *et al.*, Phys. Rev. **C44** (1991), R582.
14. I. Slaus, Y. Akaishi and H. Tanaka, Phys. Rep. **173**, 257-300 (1989).
15. T. Iijima *et al.* (KEK-E176 collaboration), Nucl. Phys. **A546** (1992) 588.
16. J.K. Ahn *et al.* (KEK-E224 collaboration), Nucl. Phys. **A625** (1997) 231.
17. C. Gobbi, C. B. Dover and A. Gal, Phys. Rev. **C50** (1994) 1594.
18. T. Fukuda *et al.* (KEK-E224 collaboration), Phys. Rev. **C58** (1998), 1306.
19. M. M. Nagels, T. A. Rijken, and J. J. de Swart, Phys. Rev. **D15** (1977), 2547.
20. B. Jakobsson *et al.*, Phys. Rev. **C44** (1991), R1238.
21. M.M. Nagels, T.A. Rijken and J.J. de Swart, Phys. Rev. **D20** (1979), 1633.
22. P.M. Maessen, T.A. Rijken and J.J. de Swart, Phys. Rev. **C40** (1989), 2226.
23. Y. Nara, Nucl. Phys. **A638** (1998) 555c; Eprint nucl-th/9802016;  
Y. Nara, N. Otuka, A. Ohnishi and T. Maruyama, Prog. Theor. Phys. Suppl. **129** (1997), 33;  
Y. Nara, N. Otuka, A. Ohnishi, K. Niita, S. Chiba, submitted, Eprint nucl-th/9904059.
24. T. Fukuda, in this proceedings.